Surface Plasmon Resonance as a Tool for the Estimation of Adsorbed Polymeric Layer Characteristics: Theoretical Considerations and Experiment

ALEXANDROS G. KOUTSIOUBAS, NIKOLAOS SPILIOPOULOS, DIMITRIOS L. ANASTASSOPOULOS, ALEXANDROS A. VRADIS, GEORGE D. PRIFTIS

Department of Physics, University of Patras, GR 26 500, Greece

Received 28 October 2006; revised 12 March 2007; accepted 12 March 2007
DOI: 10.1002/polb.21203
Published online in Wiley InterScience (www.interscience.wiley.com).

ABSTRACT: The potential application of Surface Plasmon Resonance (SPR) spectroscopy in evaluating the thickness and volume fraction of adsorbed macromolecular layers is discussed in this work. The sensitivity of SPR spectroscopy to different layer concentration and to the layer extension normal to the surface (thickness) is theoretically illustrated. A new approach for the interpretation of SPR data is presented, which is applicable whenever the functional form of the density profile is known. The use of the proposed procedure for the fitting of experimental results from PS-PEO brush self-assembly on alumina surface has allowed the determination of the layer parameters, which have been found to be in accordance with theoretical mean-field and scaling predictions, being also in good agreement with previous results from neutron reflectivity experiments. Furthermore, it has been confirmed that the dependence of the brush layer thickness d on the molecular weight M_w obeys the scaling law $d \sim {M_w}^{0.63}$. Since surface plasmon measurements can be acquired quite fast, it is suggested that under the present analysis scheme, the technique may be implemented to probe the average conformational properties of adsorbed macromolecular layers during their formation or under external stimuli. ©2007 Wiley Periodicals, Inc. J Polym Sci Part B: Polym Phys 45: 2060–2070, 2007
Keywords: adsorption; block copolymers; brush structure; interfaces; surface plasmons

INTRODUCTION

The adsorption of polymers at interfaces is a field of fundamental importance in a wide range of applications like adhesion, lubrication, and the stabilization of colloidal dispersions.[1] Furthermore macromolecular adsorption in general, is also relevant to biology in conjunction with film coatings that may modify a surface to imitate interesting biological interfaces. These widespread applications have spurred numerous theoretical and experimental investigations on the subject for over 35 years.

A very interesting model system that has received much attention is the one that concerns terminally grafted polymers or polyelectrolytes onto a solid surface, especially the case of brush formation where the grafting density is so high that leads to strong overlap between the chains and elongation normal to the surface. These systems and especially A-B type block copolymer brushes formed by self assembly or the "grafting from" method have been extensively reviewed,[2,3]

Correspondence to: A. A. Vradis (E-mail: vradis@physics.upatras.gr)

Journal of Polymer Science: Part B: Polymer Physics, Vol. 45, 2060–2070 (2007)

while considerable experimental,[4–11] theoretical,[12–17] and computer simulation[18] effort has gone into the determination of the segment density profile as a function of coverage, molecular weight, polydispersity, solvent quality, salt concentration and so forth.

Recently many studies have focused on the effects of external stimuli, like solvent shear,[19] temperature variations,[7] applied electrical fields,[20] and ionic strength variations,[21] to the conformational properties of polymer brushes and other relative systems. Potentially, control of the brush layer response to environmental changes, may lead to surfaces with switchable properties that is, "smart surfaces."[22]

Various experimental techniques have been employed to determine the properties of polymer brushes on solid surfaces, such as neutron scattering[5,6] and reflectivity,[7–11] direct surface force measurements,[23,24] hydrodynamic methods,[25] multiple angle ellipsometry,[21] evanescent wave ellipsometry,[26] and quartz crystal resonance.[27] Among them the most accurate and commonly used method that may also yield the detailed structure (volume fraction profile) of the brush layer is neutron scattering mainly because sources of small wavelength as "fast" neutrons, generally provide better experimental resolution. However as neutron sources are not readily available in the lab and the measurement procedure is relatively time consuming it is hard to follow the dynamics of conformational changes in real time.

In the present work we examine the potential effectiveness of the Surface Plasmon Resonance Spectroscopy (SPRS) as a fast complementary technique for the study of the conformations of self-assembled polymer brushes. Since the theoretical prediction[28] and first experimental observation[29] of surface plasmons (SP), many experimental methods based on the extremely sensitive characteristics of SP have emerged, focusing on the study of surface effects. In particular the optical excitation of SP by evanescent waves under the Kretschmann configuration[30] has been used for *in situ* adsorption studies of self-assembled monolayers,[31] polymer adsorption on metal or chemically altered surfaces[32–37] and in many biological applications such as protein interactions, lipid bilayers, tissue engineering, cell adhesion on biomaterial surfaces, and antigen-antibody binding.[38] Furthermore many useful techniques based on the optical excitation of SP were introduced as surface plasmon microscopy,[39] surface plasmon waveguide spectroscopy[40] and surface plasmon field-enhanced fluorescence spectroscopy.[41]

With the exception of a few cases,[42] most SP-related works in the literature focus solely on the measurement of adsorbed amounts. This is due to the fact that with any optical based probe, the response is depended on both thickness and dielectric constant variation of the layer under investigation. The separation of these two convoluted contributions is a quite challenging task especially in the case where the layer comprises of a very small number of molecules and is non light absorbing (transparent).[43] In these cases alternative methods have been proposed that involve multiple wavelength measurements[44,45] or combinations of different surrounding mediums[46,47] that unfortunately limit the applicability of the technique.

It has been shown[48] that for very thick adsorbed layers (above 0.5 μm) the density profile can be determined by ellipsometric measurements. Recently, Toomey et al.[49] have demonstrated that under certain experimental conditions and analysis scheme, ellipsometry, can monitor *in situ* the adsorbed amount and thickness of self-assembled polystyrene-poly (vinyl pyridine) block copolymer brushes, adsorbed on silicon oxide surfaces from toluene. Also Sarkar and Somasundaran[50] have related changes in the response of SP with conformational changes of Poly(acrylic acid) immobilized on gold surfaces under pH variation.

In this work we present numerical calculations on the effect of different adsorbed layer conformations on the SP response. These calculations are checked by fitting SPR experimental results from adsorbed PS-PEO diblock copolymer layers on alumina surfaces. It is shown that the SPR curve is sensitive to different conformations of the adsorbed layer for thicknesses above 20 nm, but the technique cannot resolve the detailed functional form of the volume fraction profile. The term "conformation" that is used throughout this text, refers to different extensions and approximate concentrations of the adsorbed polymeric layer. Details on the experimental data treatment are presented, together with a discussion of the accuracy that can be obtained and the potential use of this analysis in a wide range of studies where time resolved information for the adsorbed layer extension and concentration is required, as for example, in the case of self-assembly dynamics and external stimuli response.

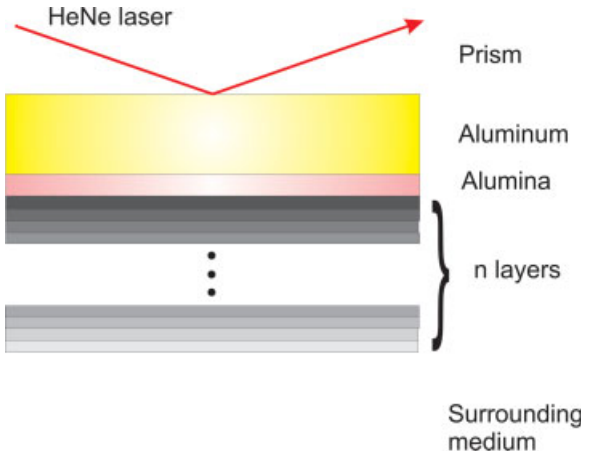

Figure 1. Generalized stacked layer model of the optical system under study. [Color figure can be viewed in the online issue, which is available at www.interscience.wiley.com.]

THEORETICAL CONSIDERATIONS

Free electrons on a metal boundary can, under certain conditions, perform coherent oscillations which are called SP. These oscillations are electromagnetic waves that propagate along the interface between a metal and its dielectric environment. A comprehensive review of SP physics is given in the book by Raether.[51]

The optical excitation of SP may be triggered by an evanescent electromagnetic wave, generated by light incident on a medium such as a metal-coated glass prism under total internal reflection conditions. This configuration was first proposed by Kretschmann et al.[30] At a particular incidence angle the wavevector of the evanescent electromagnetic field matches the SP wavevector, inducing oscillations of the free electron gas of the metal. This resonance interaction is observed as a sharp minimum in the reflectance due to the energy transfer from photons to SP.

For practical applications of SPR, it is essential that the valence electrons of the metal film in contact with the prism should exhibit a "gas-like" behavior. This requirement leaves a few candidates for the excitation of SP and in practice only silver, gold, and most rarely aluminum thin films have been used.

The quantitative description of the reflected intensity versus the angle of incidence (SPR curve) can be described by Fresnel's equations or in a more compact way by the matrix formalism for homogeneous stratified dielectric media.[52] The system is modeled as a stack of optically homogeneous layers that are characterized by their thickness and complex dielectric constant (Fig. 1). The first layer is the prism, while the last layer is the bulk surrounding medium, that are both treated as semi-infinite. In the simplest case, between these two layers only one additional thin metal layer is present.

The shape of the SPR curve is characterized by four major parameters: the critical angle θ_c, the angular position of the minimum θ_{min}, the minimum reflection intensity R_{min} and the half-width $\theta_{1/2}$ (Fig. 2). The critical angle depends solely on the refractive indices of the prism and surrounding medium while all other parameters are dependent on the properties of each layer.

In the case of an additional layer on top of the metal film, the SPR curve is altered. Based on this fact many SP-based applications have emerged to measure the adsorption of polymers[32–37] or other surface interactions.[31,38] Because of the extremely sensitive response of the SPR curve, even subnanometer layers could be resolved. The maximum probing depth is about 200 nm due to the exponentially decaying nature of the evanescent field.

As in the case of ellipsometry, the sensitivity of the SPR technique refers to the "optical thickness" of the layer under study. However the "optical thickness" is a composite quantity including both layer thickness and dielectric constant contributions. The identification of these two parameters from a measured "optical thickness" is very difficult for layers that are transparent (real dielectric constant) and impossible for layers thinner than 20 nm.[44] Salamon et al.[43] have shown that in the case where the layer

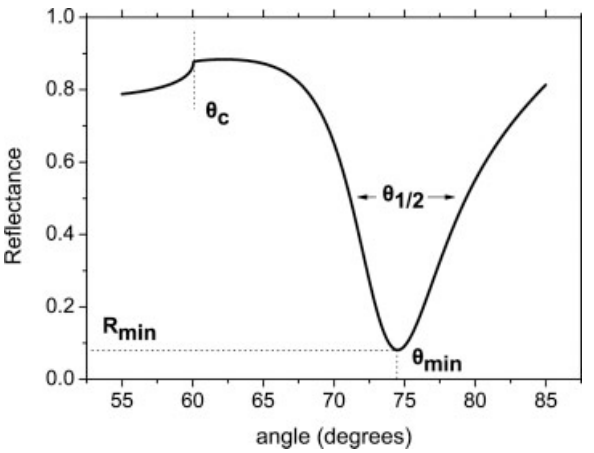

Figure 2. Key properties of the SPR curve for a prism/gold/toluene system (see text).

under study is light absorbing (non zero imaginary part of the dielectric constant) the estimation of its thickness and dielectric constant is much simplified.

Considering the system prism/metal/transparent layer/surrounding medium, the main effect on the shape of the SPR curve due to the thin transparent layer is a shift of $\theta_{\min}$. To a first approximation[53] this shift is given by

$$\Delta(\sin\theta_{\min}) = \varepsilon_0^{-1/2}\left(\frac{\varepsilon_2-\varepsilon_n}{\varepsilon_2}\right)\left(\frac{\varepsilon_1'\varepsilon_n}{\varepsilon_1'+\varepsilon_n}\right)\left(\frac{\varepsilon_2-\varepsilon_1'}{\varepsilon_n-\varepsilon_1'}\right)(-\varepsilon_1'\varepsilon_n)^{-1/2}\left(\frac{2\pi d_2}{\lambda}\right) \quad (1)$$

where ε_0 the real dielectric constant of the prism, $\underline{\varepsilon_1} = \varepsilon_1' + i\varepsilon_1''$ the complex dielectric constant of the metal, ε_2 the real dielectric constant of the coating layer, ε_n the real dielectric constant of the surrounding medium, d_2 the thickness of the coating and λ the wavelength of the incident light beam. Obviously a certain shift of $\theta_{\min}$ can be produced by infinite pairs of (ε_2,d_2), so from this single information, it is not possible to deduce the values of thickness and dielectric constant of the coating layer.

Apart from $\theta_{\min}$, two other parameters of the SPR curve, namely $R_{\min}$ and $\theta_{1/2}$ may yield useful information. However, for a transparent coating, different pairs of (ε_2,d_2) give a negligible effect on $R_{\min}$.[51] On the contrary the half-width of the SPR curve $\theta_{1/2}$ has different values for each pair of (ε_2,d_2). This is due to the fact that the presence of the transparent layer changes the electromagnetic field distribution propagating inside the metal film and surrounding medium. With growing "optical thickness" of the layer, the field flow in the metal substrate grows, leading to increased damping of SP or in other words, to bigger half-width of the SPR curve. Thus, in principle, if this change in $\theta_{1/2}$ is large enough to be experimentally measurable, one may obtain the values of ε_2, d_2.

An analytical expression based on a second order approximation[53] that relates $\theta_{1/2}$ to ε_2, d_2 is quite complex while it does not provide sufficiently accurate results. This is because the magnitude of $\theta_{1/2}$ depends also on higher order effects. It is for this reason that detailed numerical calculations were carried out, using the matrix formalism[52] for the calculation of SPR curves.

Since we are interested in the case of non light absorbing layers of terminally adsorbed polymers that have typical thicknesses above 20 nm,[9] we initially performed numerical calculations involving the above-mentioned quantities for the four layer system, prism ($\varepsilon_0 = 2.97$)/gold ($\underline{\varepsilon_1} = -11 + i1.46$, $d_1 = 50$ nm)/polystyrene brush layer (ε_2,d_2)/solvent–toluene ($\varepsilon_{\text{solvent}} = 2.23$). For polystyrene we have $\varepsilon_{\text{polymer}} = 2.50$. All given values for the optical properties of each material are valid for the used laser beam wavelength $\lambda = 632.8$ nm.

Initially the polymer layer volume fraction is considered as a step function with uniform polymer concentration. It is also assumed that the dielectric constant varies linearly with the polymer fractional volume.[31] That means that the dielectric constant of the adsorbed layer is approximated as $\varepsilon_2 = V_{\text{solvent}} \cdot \varepsilon_{\text{solvent}} + V_{\text{polymer}}\ \varepsilon_{\text{polymer}}$, where $\varepsilon_{\text{solvent}}$, $\varepsilon_{\text{polymer}}$ the dielectric constants and V_{solvent}, V_{polymer} the fractional volumes occupied by the solvent and polymer, respectively.

Let us assume that a measurement on this system yields a shift in $\theta_{\min}$ equal to 0.50° after the formation of a polystyrene brush on the gold surface.[54] In Figure 3(a) we present numerical calculations, which provide all possible (ε_2,d_2) pairs for $\Delta\theta_{\min} = 0.50^\circ$. Then for each one of these pairs we calculate $\Delta\theta_{1.2}$ and plot it against d_2 [Fig. 3(b)]. As it was mentioned, each pair corresponds to a different $\Delta\theta_{1/2}$ making it possible to distinguish the correct pair (ε_2,d_2).

The dependence of $\Delta\theta_{1/2}$ on d_2 appears to be approximately linear with a small slope equal to $\approx -5 \cdot 10^{-4}$ degrees/nm. This slope and the SPR apparatus resolution[55] are the two factors limiting the experimental accuracy. In the present case if there is a $\pm 0.005^\circ$ experimental error in the determination of $\theta_{1/2}$, then the error in d_2 is estimated to be about ± 10 nm, while for $\pm 0.0005^\circ$ error in $\theta_{1/2}$ the accuracy is improved by one order of magnitude being equal to ± 1 nm. The error associated with the dielectric constant of the polymer layer is related to the error in d_2 [Fig. 3(a)]. As mentioned above when the thickness of the layer under study is below 20 nm, the error in ε_2 rises considerably, making the estimation of the adsorbed layer parameters impossible.

The key factor influencing the magnitude of the slope in Figure 3(b) is $\Delta\theta_{\min}$, which corresponds to the amount of adsorbed polymer. So, for very concentrated and long brushes we expect improved measurement accuracy because the magnitude of the slope in Figure 3(b)

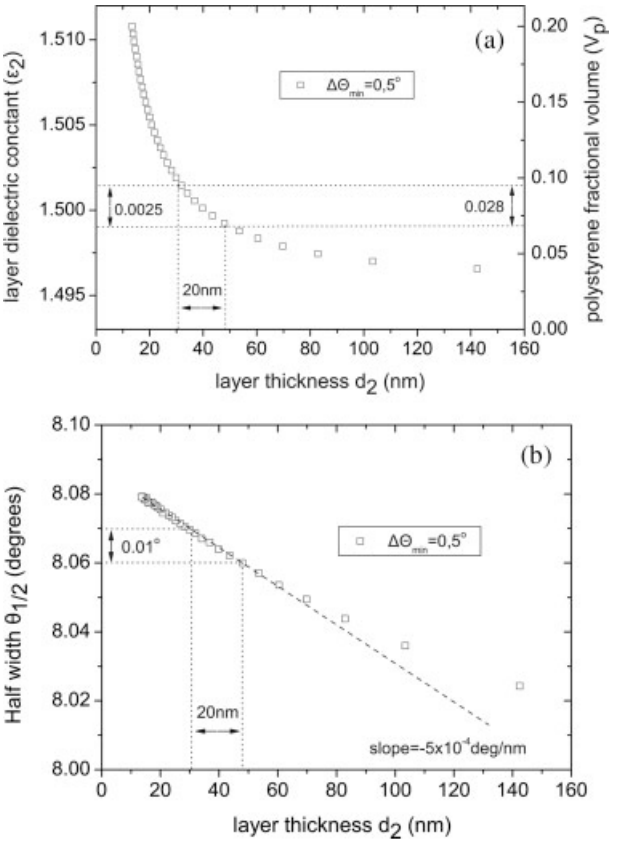

Figure 3. (a) Numerical calculation of (ε_2, d_2) pairs corresponding to $\Delta\theta_{min} = 0.50$ for the prism/gold/PS layer/toluene system described in the theoretical section. (b) SPR curve half widths corresponding to different (ε_2, d_2) pairs, plotted against d_2. Dotted lines determine the approximate error margins corresponding to a hypothetical experimental error in $\theta_{1/2}$ equal to $\pm 0.005^\circ$.

increases and consequently the change in $\Delta\theta_{1/2}$ is easily detected. It should be mentioned that this fact limits the applicability of the method only for very short or dilute polystyrene layers in toluene that are characterized by a coverage below 1 mg/m^2, depending of course on the apparatus resolution. Self-assembled brushes[9] have typical coverages above 1 mg/m^2 while chemically grafted brushes[7] may produce coverages above 10 mg/m^2.

Apart from gold, we performed calculations involving excitation of SP on silver and aluminum thin films. For aluminum [Fig. 4(a) and 4(b)] we found comparable results concerning the possible attainable experimental accuracy while for silver it was found that the dependence of $\Delta\theta_{1/2}$ on different (ε_2,d_2) pairs is weaker by a factor of two compared to gold or aluminum, mainly due to the low imaginary part of the dielectric constant of silver. Therefore gold or aluminum films are the best choice for this kind of investigations.

Now we turn to the more general case where the polymer volume fraction is not constant throughout the layer length d_0 and is characterized by a specific functional form $V(z)$. Although SPR technique is unable to determine the functional form of the volume fraction profile, when an underlying theory (or complementary information from other experimental techniques) about the form of the adsorbed layer is available, then with the proposed method it is possible to deduce the parameters of the model from SPR measurements.

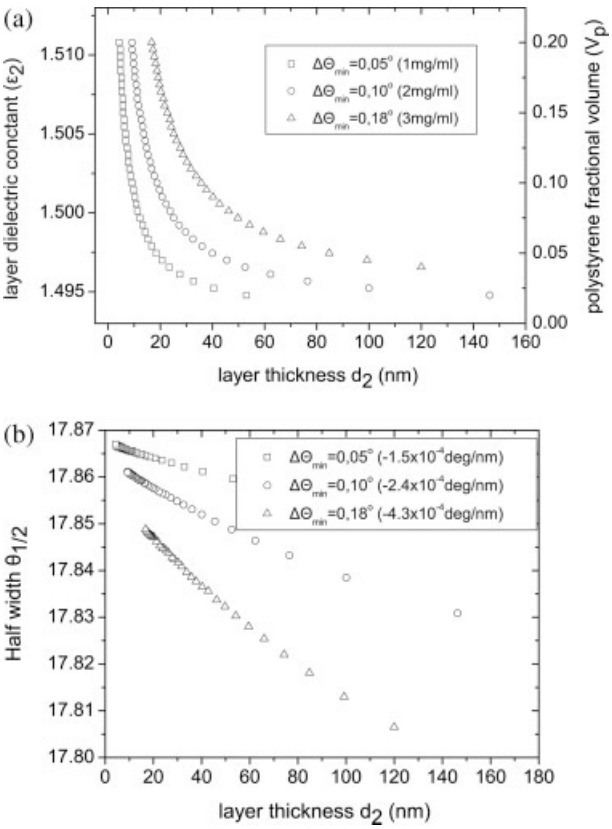

Figure 4. (a) Numerical calculation of (ε_2, d_2) pairs corresponding to various shifts of θ_{min} for the five layer system prism ($\varepsilon_0 = 2.97$)/aluminum ($\varepsilon_1 = -49 + i19.7$, $d_1 = 15$ nm)/alumina-Al_2O_3 ($\varepsilon_{oxide} = 2.6$, $d_{oxide} = 3$ nm)/polystyrene brush layer (ε_2, d_2)/toluene ($\varepsilon_s = 2.23$). The values in parenthesis give typical adsorbed amounts of polystyrene brushes that produce the respective $\Delta\theta_{min}$. (b) SPR curve half widths that correspond to different (ε_2, d_2) pairs, plotted against d_2. It is evident that high adsorption amounts tend to produce bigger changes in $\theta_{1/2}$ (the values in parenthesis give the approximate slope).

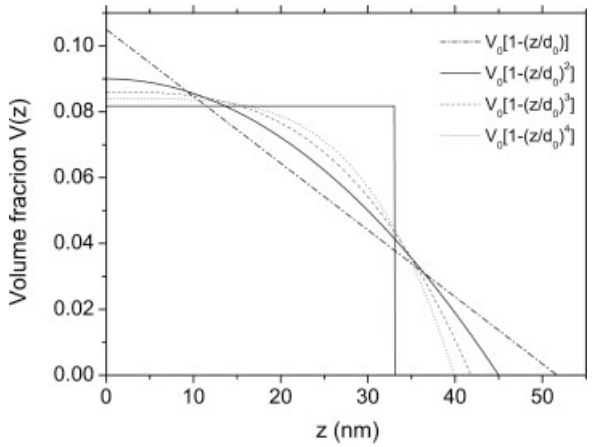

Figure 5. Fitting of a parabolic layer profile (full line) using several other functional forms.

In the case of A–B type block copolymer brushes, theory, simulation and experiment suggest that above a certain grafting density the volume fraction profile has a parabolic form.[11]

$$V(z) = V_0\left(1 - \frac{z^2}{d_0^2}\right) \tag{2}$$

where z is the distance normal to the surface, V_0 is the polymer fractional volume on the surface and d_0 is the thickness of the brush layer. For the modeling of such systems we divided the total profile in multiple layers n of constant thickness d_0/n, each one having polymer fractional volume that is strictly defined by the layer's parameters and the profile's functional form. Thus, each layer is characterized by a pair of V_p and d_p. These values are inserted in the Fresnel equations and produce a reflectivity curve, which is in turn compared to the experimental one. Then using a Simplex least squares method, the best fit criteria (minimum in the sum of squared deviations) determine the final V_{0p} and d_{0p} values. Obviously the above method can be used for any function describing the volume fraction profile such as exponential or power law.

It is also of interest to examine the case where a reflectivity curve that is produced by an adsorbed parabolic profile is fitted using different functional profiles. Using the above-mentioned method, with step and power law profiles ($V(z) = V_0[1 - (z/d_0)^n]$ with $n = 1\ldots4$) as trial functions instead of the known parabola, we obtained equally good fits resulting in almost the same estimation for the total adsorbed amounts. However they give different estimations for the layer extension and volume fraction. These facts are illustrated in Figure 5 where an SPR curve deduced by a parabolic profile (as has been taken from a previous neutron reflectivity study[9]) is fitted using a step function and different functional forms of the layer volume fraction profile. While the estimation of the total adsorbed amount is accurate enough for all cases, there are significant errors in V_0 and d_0 which especially for d_0 can be as large as 30% in the case of the step function profile.

Since the vast majority of real adsorbed polymeric layers largely deviate from a step profile form, it is evident that the commonly used step profile functions for the fit of SPR data may result in large errors in the estimation of the other two parameters V_0,d_0. These theoretical considerations are checked experimentally in the following sections.

EXPERIMENTAL

An extensive description of the SPR apparatus, sample preparation and experimental procedure is given in a previous publication.[37] Briefly, for these experiments, we used a custom made SPR apparatus in the Kretschmann[30] configuration. SP are excited by a p-polarized laser beam (λ = 632.8 nm) on thin ($\approx$ 15 nm) aluminum films prepared by vacuum evaporation on the face of an optically flat SF10 high refractive index (n = 1.7230) equilateral prism. The copolymer adsorption from toluene solutions is studied on the ultra-thin ($\approx$ 3 nm) naturally occurring oxide layer (alumina-Al_2O_3) formed on freshly evaporated aluminum films upon contact with the ambient atmosphere.

A custom made $\theta - 2\theta$ goniometer driven by two precision stepper motors was used to perform scans of the intensity of the reflected beam as a function of the incidence angle (SPR curve). A beam splitter is placed between the laser source and the sample to monitor the source light intensity. The intensity of the source and reflected beams were measured with the aid of two photodiodes whose output was transmitted to a DSP module and on a PC for data processing and storage. Normalized SPR curves were obtained by dividing the reflectivity of p-polarized light by that of s-polarized light. Because s-polarized light does not excite SP, such normalization corrects any errors caused by the optical components and scanning procedure.[36]

Table 1. Characterization of Copolymers Used in This Study

Copolymer	Molecular Weight (M_W)	PEO Content % wt	Polydispersity (M_w/M_n)
PS-PEO 80 K	80,000	5.0	1.07
PS-PEO 182.7 K	182,700	4.2	1.07
PS-PEO 322 K	322,000	2.4	1.19
PS-PEO 496.7 K	496,700	1.2	1.18

Solvent and polymer solutions where placed in a custom made PTFE cell, which is sealed with the aid of a PTFE O-ring pressed against the aluminum coated face of the prism. The temperature inside the cell was monitored by a PTFE coated thermocouple with a precision of ± 0.1 °C. Four diblock copolymers of polystyrene-*b*-polyethylene oxide (supplied from Polymer Laboratories) were used in this study. Their molecular weight and other characteristics are summarized in Table 1.

After each evaporation procedure the samples were stored for at least 3 days in a specimen box left in the laboratory environment to ensure the complete formation of a stable oxide layer over the aluminum surface. Then the prism was attached to the PTFE cell and placed on the rotating sample stage of the goniometer.

First, the cell was filled with 10 mL of fresh toluene (P.A. quality) and the SPR curve was recorded every 10 min for about 1 h. These experimental SPR curves were fitted to a four-layer model (prism/aluminum/alumina/toluene) where the refractive index of toluene is set according to the measured temperature.[37] Typical values of the dielectric constants found were $\varepsilon_{Al} = -49.8 + i19.7$ and $\varepsilon Al_2O_3 = 2.6$ while the thickness of the aluminum layer was 3.1 ± 0.2 nm. When no significant change to the fitting results (more than 1%) was observed over a period of 1 h, 5 mL of PS-PEO copolymer solution (0.3 mg/mL) was added into the cell to obtain a final concentration of 0.1 mg/mL. It is known[56] that at this concentration the copolymers are not in a micellar state. After the injection of the copolymer solution into the cell, changes in the SPR curve were measured every 10 min for 4 h. Each reflectivity scan covers 14°, from 62° to 76°.

Data Analysis

To determine the characteristics of the brush layer, the values of dielectric constants and thicknesses of the aluminum and alumina films were kept fixed to the values measured before solution injection. Two fitting models were used:

a. A five-layer model (prism/aluminum/alumina/brush layer/solution) where the brush layer is treated as a step of thickness d_{0s} and constant polymer fractional volume V_{0s}

b. A 14-layer model (prism/aluminum/alumina/brush 10-layers/solution) where the volume fraction of the brush layer possesses a parabolic functional dependence that is approximated by ten layers[57] of equal thickness d/n and varying polymer fractional volume according to eq (2).

In the first fitting model the thickness d_{0s} and fractional volume V_{0s} of the step layer are left as free parameters while in the second model the fractional volume at the surface V_{0p} and the parabola thickness d_{0p} (eq 2) are the two parameters determined by the fit. In both cases no extra constraints were imposed to the fitting parameters.

In all calculations the refractive index of the copolymer chains is set equal to $n_{polymer} = 1.582$. Also the effect of non zero copolymer concentration contribution to the refractive index of the bulk solution is taken into account.[37] All fitting algorithms used, were developed in Fortran language, implementing the Simplex least squares fitting method that has been previously used for the analysis of neutron reflectivity data.[19] The root mean square of residuals of all fitted SPR curves was in the range $2.5 - 3.5 \times 10^{-4}$.

Errors in the experimentally determined SPR curve come mainly from the following sources: laser intensity fluctuations, noise in the photo detectors and related electronics, positioning uncertainty related to the limited accuracy of the goniometer and uncertainty related to the precision of the solution temperature measurement. Calculations for the present experimental setup and angle scan range, summing up the contribution of all these factors give a $\pm 0.002°$ error in θ_{min} and a $\pm 0.008°$ error in $\theta_{1/2}$. It was found that errors in the measured temperature mainly affect the position of the curve minimum while laser intensity fluctuations raise the errors in the determination of the curve half width.

RESULTS AND DISCUSSION

The main result drawn from the numerical analysis presented in the theoretical section is that quantitative information for the structural

Table 2. Results of Fitted SPR Measurements

PS-PEO M_w	Γ_p (mg/m^2)	R_g (nm)	σ^*	s (nm)	V_{0p}	d_{0p} (nm)	V_{0s}	d_{0s} (nm)
80 K	3.58 ± 0.02	9.7	7.9	6.1	0.150 ± 0.019	36.4 ± 5.3	0.135 ± 0.018	27.1 ± 4.4
182.7 K	3.08 ± 0.02	15.8	8.0	9.9	0.095 ± 0.014	49.5 ± 7.5	0.086 ± 0.013	36.5 ± 5.8
322 K	2.60 ± 0.02	22.1	7.5	14.3	0.046 ± 0.006	85.0 ± 10.4	0.042 ± 0.006	61.9 ± 8.3
496.7 K	2.07 ± 0.01	28.7	6.6	19.8	0.028 ± 0.004	111.4 ± 16.0	0.027 ± 0.004	79.4 ± 12.1

Γ_p adsorbed amount parabola model, R_g radius of gyrAtion, σ^* reduced coverage, s interanchor distance, d_{0p} parabolic profile thickness, V_{0p} volume fraction of the parabolic profile on the surface, d_{0s} step profile thickness, V_{0s} step profile fractional volume on the surface.

parameters of adsorbed layers can be extracted from SPR measurements. This is true, especially for the systems under investigation where adsorbed polymers form polymeric brushes with a known profile form.

In a previous SPR study[37] we have studied the kinetics of PS-PEO brush formation at the alumina/toluene interface. It was found that the PS block has a negligible affinity for the alumina surface but on the contrary the PEO block anchors the copolymer chain on the surface. Kinetic rate factors and final adsorption amounts observed where typical for self-assembled brush layers.

To check the theoretical analysis, we chose to study the conformational properties of self-assembled PS-PEO diblock copolymer brushes formed on the alumina/toluene interface. By fitting experimental SPR curves produced by adsorption of four different PS-PEO copolymers on alumina surfaces, we estimate the brush thickness, surface coverage and concentration.

The experimental results for the adsorption of all four copolymers have shown that at a maximum of 2 h after the solution injection in the cell, the adsorbed amount reaches a plateau value, marking the completion of the self-assembly process. Therefore only SPR curves acquired after this 2 h threshold were fitted using the two models (step-parabola) as described in the experimental section. The obtained results for each copolymer and other related quantities as the reduced coverage σ^* and interanchor distance s[58] are presented in Table 2.

A straightforward comparison of the fitted experimental results for the three copolymers of 80 K, 182.7 K, and 497 K molecular weight with previously published neutron reflectivity data[9] cannot be made because the total adsorption in each case is not the same due to differences in the PEO-SiO_2 and PEO-alumina interaction energy. However, the layer thicknesses d_{0p} and volume fractions on the surface V_{0p} obtained by SPR are of the same order of magnitude as those determined from neutron reflectivity data, while the same qualitative behavior is found for the dependence of V_{0p}, d_{0p} on the molecular weight M_w.

Mean field[60] and scaling theory[13] predict that for self-assembled brushes of end tethered asymmetric diblock copolymers, where the interanchor distance is fixed, the layer thickness varies linearly with M_w. However, in the present case the interanchor distance varies for each layer and only the interaction energy between the PEO anchor block and the surface is approximately fixed, since all used copolymers have comparable PEO chain lengths (Table 1). Under these conditions the layer thickness is expected to vary with $M_w^{3/5}$.[61] This is a result that has been verified for PS-PEO brush self-assembly on quartz and mica surfaces using neutron reflectivity[9] and surface force measurements,[24] respectively.

In Figure 6, the thickness of each copolymer layer versus molecular weight is plotted in the case of parabola fitting model. It is evident that despite their lower surface coverage, chains of

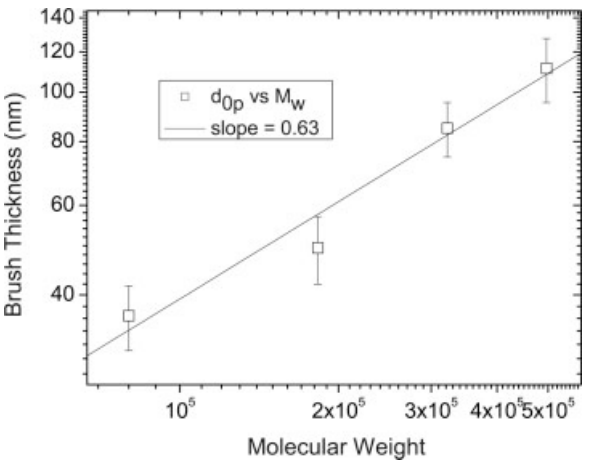

Figure 6. Experimentally determined thickness of brush layers plotted against molecular weight for each copolymer.

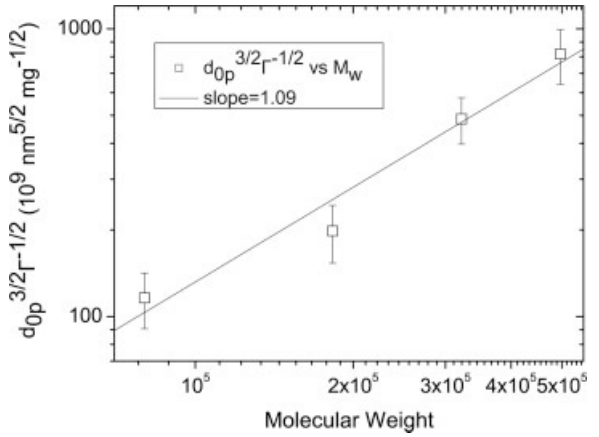

Figure 7. Scaling of $d_{0p}^{3/2}\Gamma^{-1/2}$ with molecular weight M_w.

higher molecular weight tend to produce longer brush layers. The linear behavior in this log–log plot reveals a power law $d_{0p} \sim M_w^{0.63\pm0.11}$ that is in agreement with the above-mentioned theoretical result.

Also, for a variable surface density both scaling[13] and mean field calculations[60] predict that the product $d_{0p}s^{2/3}$ or equivalently $d_{0p}^{3/2}\Gamma^{-1/2}$ varies linearly with copolymer molecular weight M_w. In Figure 7, a scaling plot of $d_{0p}^{3/2}\Gamma^{-1/2}$ versus M_w is presented. The obtained slope 1.09 $\pm$ 0.17 is quite close to 1, as predicted by the mean field theoretical calculations.

This quantitative and qualitative agreement in the results both with theory and previous experiments, demonstrates that the SPRS, under the adopted data analysis scheme can approximate the length and the average concentration of a polymer brush layer. This is accomplished by assuming a parabolic functional dependence of the volume fraction profile that is justified since the values of the calculated inter-anchor distance and reduced coverage suggest strong overlap between PS chains (brush regime[11]).

The error bars in Figure 6 are calculated using all fitted SPR curves that were acquired 2 h after the initiation of each adsorption experiment. The magnitude of these error bars is in accordance with expectations based on the theoretical analysis and the resolution of the present SPR apparatus.

In the case where no assumptions are made about the functional dependence of the volume fraction profile and a step function is used, the obtained results (Table 2) give a good estimate of the total adsorbed amount Γ but the volume fraction V_{0s} and especially the thickness d_{0s} of the brush layer are systematically underestimated. This fact should be taken into account in the interpretation of SPR experiments involving macromolecular adsorption on surfaces.

As described in the theoretical section, an apparatus possessing better resolution is expected to be capable of measurements of both thickness and fractional volume with adequate precision during the self-assembly procedure. This kind of measurements could be very helpful to realize whether the equilibrium layer structure is determined from equilibrium arguments only or if it is dominated by kinetic issues.[49]

In conjunction with recent advances in the experimental implementation of SPRS,[36,62,63] the evolution of the adsorbed layer may be monitored with enhanced accuracy and time resolution. Furthermore, the use of self-assembled or deposited thin coatings[64] on the metal surface, may expand the applicability of the method to imitate surface chemistries that are also studied by other experimental techniques.

Finally, it should be pointed out that the overall resolution of the technique, except for the experimental setup accuracy, is highly dependent on the optical contrast between the solvent and the macromolecule under investigation. In the present case the refractive indices of toluene and polystyrene have a relatively small difference ($\Delta n = n_{\text{polystyrene}} - n_{\text{toluene}} = 0.09$). For higher differences between these two refractive indices, improved sensitivity of the SPRS technique is expected. For example in the case of water soluble polymers ($\Delta n \approx 0.2$), theoretical calculations predict improved accuracy by a factor of two in the determination of the conformational properties of adsorbed layers. This result is very important for polyelectrolyte and biomolecular adsorption, because this class of macromolecules is water soluble.

CONCLUSIONS

Despite the fact that SPRS is a widely used technique in the study of macromolecular systems near solid/liquid interfaces, most reported applications focus on measuring adsorbed amounts at equilibrium or rate factors of adsorption kinetics. The present work demonstrates that by presumption of functional form of the density profile, SPRS may successfully

approximate the volume fraction and thickness of surface adsorbed macromolecular layers.

We have conducted an analysis on the experimental accuracy that can be achieved depending on the overall SPR apparatus resolution. The experimental investigation of end-tethered PS-PEO copolymer brushes on alumina, provided results that are consistent with theory and previous neutron reflectivity and surface force data. In combination with the potential high temporal resolution of the technique, one may acquire real time information concerning the approximate density and extension of polymeric layers during the assembly procedure or under external stimuli. It is shown that gold or aluminum metal thin films are the optimum choices for this kind of investigations. It is predicted that in the case of water-soluble macromolecules the applicability of the technique is enhanced due to higher optical contrast. Finally the current numerical analysis suggests that the step profile functions, commonly used for the interpretation of SPR data, leads to a large systematic underestimation of the layer extension and volume fraction.

The authors thank Professor Chris Toprakcioglu for helpful discussions and comments on the manuscript.

REFERENCES AND NOTES

1. Polymeric Stabilization of Colloidal Dispersions; Napper, D. H., Ed.; Academic Press: London, 1983.
2. Polymers at Interfaces; Fleer, G. J.; Cohen Stuart, M. A.; Scheutjens, J. M. H. M.; Cosgrove, T.; Vincent, B., Eds.; Chapman & Hall: Bristol, 1993.
3. Polymer Brushes: Synthesis, Characterization, Applications; Advincula, R. C.; Brittain, W. J.; Caster, K. C.; Rühe J., Eds.; Wiley: Hoboken, NJ, 2004.
4. Taunton, H. J.; Toprakcioglu, C.; Fetters, L. J.; Klein, J. Nature 1998, 332, 712–714.
5. Auroy, P.; Auvray, L.; Leger, L. Phys Rev Lett 1991, 66, 719–722.
6. Auroy, P.; Mir, Y.; Auvray, L. Phys Rev Lett 1992, 69, 93–95.
7. Karim, A.; Satija, S. K.; Douglas, J. F.; Anker, J. F.; Fetters, L. J. Phys Rev Lett 1994, 73, 3407–3410.
8. Perahia, D.; Wiesler, D. G.; Satija, S. K.; Fetters, L. J.; Sinha, S. K.; Milner, S. T. Phys Rev Lett 1994, 72, 100–103.
9. Field, J. B.; Toprakcioglu, C.; Ball, R. C.; Stanley, H. B.; Dai, L.; Barford, W.; Penfold, J.; Smith, G.; Hamilton, W. Macromolecules 1992, 25, 434–439.
10. Kent, M. S.; Lee, L. T.; Farnoux, B.; Rondelez, F. Macromolecules 1992, 25, 6240–6247.
11. Baranowski, R.; Whitmore, M. P. J Chem Phys 1995, 103, 2343–2353.
12. Rühe, J.; Ballauf, M.; Biesalski, M.; et al. Adv Polym Sci 2004, 165, 79–150.
13. Alexander, S. J Phys 1977, 38, 983–987.
14. de Gennes, P. G. Macromolecules 1980, 13, 1069–1075.
15. Milner, S. T.; Witten, T. A.; Gates, M. Macromolecules 1988, 21, 2610–2619.
16. Halperin, A.; Tirrell, M.; Lodge, T. P. Adv Polym Sci 1991, 100, 31–71.
17. Zhulina, E. B.; Borisov, O. V.; Brombacher, L. Macromolecules 1991, 24, 4679–4690.
18. Monte Carlo and Molecular Dynamics Simulations in Polymer Science; Binder, K., Ed.; Oxford University Press: New York, 1995.
19. Baker, S. M.; Smith, G. S.; Anastassopoulos, D. L.; Toprakcioglu, C.; Vradis, A. A.; Bucknall, D. G. Macromolecules 2000, 33, 1120–1122.
20. Rant, U.; Arinaga, K.; Fujita, S.; Yokoyama, N.; Abstreiter, G.; Tornow, M. Nano Lett 2004, 4, 2441–2445.
21. Biesalski, M.; Johannsmann, D.; Ruhe, J. J Chem Phys 2004, 120, 8807–8814.
22. Anastasiadis, S. H.; Retsos, H.; Pispas, S.; Hadjichristidis, N.; Neophytides, S. Macromolecules 2003, 36, 1994–1999.
23. Hadziioannou, G.; Patel, S.; Granick, S.; Tirrell, M. J Am Chem Soc 1986, 108, 2869–2876.
24. Taunton, H. J.; Toprakcioglu, C.; Fetters, L. J.; Klein, J. Macromolecules 1990, 23, 571–580.
25. Cohen Stuart, M. A.; Waajen, F. H. W. H.; Cosgrove, T.; Vincent, B.; Crowley, T. L. Macromolecules 1984, 17, 1825–1830.
26. Kim, M. W.; Peiffer, D. G.; Chen, W.; Hsiung, H.; Rasing, T.; Shen, Y. R. Macromolecules 1989, 22, 2682–2685.
27. Domack, A.; Prucker, O.; Ruhe, J.; Johannsmann, D. Phys Rev E 1997, 56, 680–689.
28. Ritchie, R. H. Phys Rev 1957, 106, 874–881.
29. Powell, C. J.; Swan, J. B. Phys Rev 1959, 115, 869–875.
30. Kretschmann, H.; Raether, H. Z Naturforsch A: Phys Sci 1968, 23, 2135–2136.
31. Peterlinz, K. A.; Georgiadis, R. Langmuir 1995, 12, 4731–4740.
32. Knoll, W. Optical characterization of organic thin films and intefaces with evanescent waves. MRS Bull 1991, 16, 29–33.
33. Tassin, J. F.; Siemens, R. L.; Tang, W. T.; Hadziioannou, G.; Swalen, J. D.; Smith, B.; J Phys Chem 1989, 93, 2106–2111.
34. Advicula, R.; Aust, E.; Meyer, W.; Knoll, W. Langmuir 1996, 12, 3536–3540.
35. Green, R. J.; Tasker, S.; Davies, J.; Davies, M. C.; Roberts, C. J.; Tendler, S. J. B. Langmuir 1997, 13, 6510–6515.
36. Huang, Y.-W.; Gupta, V. K. Macromolecules 2001, 34, 3757.

37. Koutsioubas, A. G.; Spiliopoulos, N.; Anastassopoulos, D.; Vradis, A. A.; Toprakcioglu, C.; Priftis, G. D. J Polym Sci Part B: Polym Phys 2006, 44, 1580–1591.
38. Green, R. J.; Frazier, R. A.; Shakesheff, K. M.; Davies, M. C.; Roberts, C. J.; Tendler, S. J. B. Biomaterials 2000, 21, 1823–1835.
39. Hickel, W.; Knoll, W. Nature 1989, 339, 186.
40. Lawall, R.; Knoll, W. J Appl Phys 1994, 76, 5764–5768.
41. Knoll, W.; Park, H.; Sinner, E.; Yao, D.; Yu, F. Surf Sci 2004, 570, 30–42.
42. Jung, L. S.; Campbell, C. T.; Chinowsky, T. M.; Mar, M. N.; Yee, S. S. Langmuir 1998, 14, 5636–5648.
43. Salamon, Z.; Macleod, H. A.; Tollin, G. Biochim Biophys Acta 1997, 1331, 117–129.
44. Peterlinz, K. A.; Georgiadis, R. Optics Commun 1996, 130, 260–266.
45. Zhou, M.; Otomo, A.; Yokoyama, S.; Mashiko, S. Thin Solid Films 2001, 393, 114–118.
46. de Bruijn, H. E.; Minor, M.; Kooyman, R. P. H.; Greve, J. Optics Commun 1993, 95, 183–188.
47. de Bruijn, H. E.; Altenburg, B. S. F.; Kooyman, R. P. H.; Greve, J Optics Commun 1991, 82, 425–432.
48. Biesalski, M.; Ruhe, J.; Johannsmann, D. J Chem Phys 1999, 111, 7029–7037.
49. Toomey, R.; Mays, J.; Tirrell, M. Macromolecules 2004, 37, 905–911.
50. Sarkar, D.; Somasundaran, P. Langmuir 2004, 20, 4657–4664.
51. Raether, H. Surface Plasmons on smooth and Rough Surfaces and Gratings; Springer-Verlag: Hamburg, 1986.
52. Born, M.; Wolf, M. Principles of Optics; Pergamon Press: London, 1959.
53. Pockrand, I. Surf Sci 1978, 72, 577.
54. A polystyrene brush characterized by a surface coverage equal to about 3 mg/m^2 is expected to produce a $\Delta\theta_{min} \approx 0.5$ for the prism/gold/brush/toluene layer system described in text.
55. The term "resolution" refers to the experimental uncertainty related to the determination of the curve minimum and half width. As it is stated in the experimental section of this work, these uncertainties are mainly dependent on the three factors (a) laser intensity fluctuations (b) temperature variations (c) goniometer positioning errors.
56. Motschmann, H.; Stamm, M.; Toprakcioglu, C. Macromolecules 1991, 24, 3681–3688.
57. In all our fitting algorithms we have aproximated the adsorbed brushes by ten layers. For all cases the algorithm converges rapidly enough and a total number of about 10 layers is already producing an accurate result. More layers are simply increasing the computational time without any significant increase in the accuracy.
58. The interanchor distance s is calculated by $s = (N_A\Gamma/M_w)^{-1/2}$ where N_A is the Avogadro's number, Γ the adsorbed amount of the brush layer and M_w the copolymer molecular weight. The radius of gyration of the PS chains in toluene is evaluated from ref. 59 $R_g = 0.0117M_w^{0.595}$ nm. The ratio of the cross sectional area of a free chain in solution to the average area per grafted chain is known as "reduced coverage" and is given by the expression $\sigma^* = \pi R_g^2/s^2$. A value of the reduced coverage $\sigma^* = 2$ marks the onset of chain overlap, while layers that are characterized by $\sigma^* > 2$ are well within the brush regime (ref. 11).
59. Roovers, J. E.; Toporowski, P. M. J Polym Sci 1980, 18, 1907–1917.
60. Milner, S. T.; Witten, T. A.; Gates, M. E. Europhys Lett 1988, 5, 413–418.
61. Marques, C. M.; Joanny, J. F.; Macromolecules 1989, 22, 1454–1458.
62. Tao, N. J.; Boussaad, S.; Huang W. L.; Arechabaleta, R. A.; D'Agnese, J. Rev Sci Instrum 1999, 70, 4656–4660.
63. Zhang, H. Q.; Boussaad, S.; Tao, H. J.; Rev Sci Instrum 2003, 74, 150–153.
64. Szunerits, S.; Boukherroub, R. Langmuir 2006, 22, 1660–1663.